

Scars of Intense Accretion Episodes at Metal-Rich White Dwarfs

J. Farihi¹, B. T. Gänsicke², M. C. Wyatt³, J. Girven², J. E. Pringle^{1,3}, A. R. King¹

¹*Department of Physics & Astronomy, University of Leicester, Leicester LE1 7RH, UK; jf123@star.le.ac.uk*

²*Department of Physics, University of Warwick, Coventry CV4 7AL, UK*

³*Institute of Astronomy, University of Cambridge, Cambridge CB3 0HA*

ABSTRACT

A re-evaluation of time-averaged accretion rates at DBZ-type white dwarfs points to historical, time-averaged rates significantly higher than the currently observed episodes at their DAZ counterparts. The difference between the ongoing, instantaneous accretion rates witnessed at DAZ white dwarfs, which often exceed 10^8 g s^{-1} , and those inferred over the past $10^5 - 10^6 \text{ yr}$ for the DBZ stars can be a few orders of magnitude, and therefore must result from high-rate episodes of tens to hundreds of years so they remain undetected to date. This paper explores the likelihood that such brief, intense accretion episodes of gas-phase material can account for existing data. For reasonable assumptions about the circumstellar gas, accretion rates approaching or exceeding 10^{15} g s^{-1} are possible, similar to rates observed in quiescent cataclysmic variables, and potentially detectable with future x-ray missions or wide-field monitoring facilities. Gaseous debris that is prone to such rapid accretion may be abundant immediately following a tidal disruption event via collisions and sublimation, or if additional bodies impinge upon an extant disk. Particulate disk matter accretes at or near the Poynting-Robertson drag rate for long periods between gas-producing events, consistent with rates inferred for dusty DAZ white dwarfs. In this picture, warm DAZ stars without infrared excesses have rates consistent with accretion from particulate disks that remain undetected. This overall picture has implications for quasi-steady state models of accretion and the derived chemical composition of asteroidal debris in DBZ white dwarfs.

Key words: accretion, accretion disks— circumstellar matter— planetary systems— stars: abundances— white dwarfs

1 INTRODUCTION

Atmospheric metals should not be present in isolated white dwarf stars with effective temperatures below roughly 25 000 K. At this stage of their evolution, radiative forces become insignificant (Chayer et al. 1995), and gravitational settling pulls elements heavier than helium into the stellar interior on timescales a few to several orders of magnitude shorter than their cooling ages (Fontaine et al. 1979). Nevertheless, white dwarfs in this temperature range exhibiting atmospheric metal absorption have been known for nearly a century, and the prototype is still the nearest single white dwarf known, vMa 2 (van Maanen 1917). At 4.4 pc, this star exemplifies a few characteristics of the metal pollution phenomenon: it is a single star and thus not accreting from a stellar or substellar companion (Farihi et al. 2008a), its location within the Local Bubble and helium-dominated atmosphere (Dufour et al. 2007) precludes accretion from interstellar material, and its age of 3 Gyr is at odds with the

persistence of metals that sink within a few Myr (Koester 2009). Combined with the above facts, the abundance patterns in stars like vMa 2 have long suggested recent accretion from material such as that found in asteroids (Sion et al. 1990; Graham et al. 1990).

Indeed, evidence is now strong that metal-polluted white dwarfs accrete from planetary debris. *Spitzer* studies have revealed circumstellar disks at a significant fraction of these stars, where the temperature profile and inferred geometry of the dust is consistent with material completely contained within the Roche limit for km-sized or larger solid bodies, with innermost disk temperatures that should rapidly sublimate solids, and drive material onto the star (Xu & Jura 2011; Farihi et al. 2009; Jura et al. 2007; von Hippel et al. 2007; Gänsicke et al. 2006; Reach et al. 2005). The favored model for the origin of this material is the tidal disruption of a large asteroid analog (Jura 2003), perturbed into a high eccentricity by an unseen body such

as a major planet (Debes et al. 2012; Bonsor et al. 2011; Debes & Sigurdsson 2002). All available mid-infrared spectroscopy reveals disk matter that is silicate-rich and carbon-poor (Jura et al. 2009; Reach et al. 2009), while stellar spectroscopy reveals atmospheric pollution by refractory-rich and volatile-poor material (Farihi et al. 2010a; Jura 2006). Critically, high-resolution optical spectroscopy of the disk-contaminated stars reveals distinctly terrestrial-like abundances (Klein et al. 2010; Zuckerman et al. 2007). Thus metal-enriched white dwarfs are astrophysical traps for exoplanetary debris, acting as detectors that can yield the bulk composition of planetary building blocks that orbit intermediate mass stars.

This paper re-examines in detail the inferred accretion rates at both hydrogen and helium atmosphere, cool white dwarfs with trace metals, referred to here as DAZ and DBZ stars respectively, based on standard spectral types. As described in Girven et al. (2012), an improved calculation method is used to place both classes on equal footing, and in doing so, the derived accretion rates, averaged over the recent history for the DBZ stars, are found to be significantly higher than the current rates observed at the DAZ stars. This work explores these issues in detail and develops a model to address the observations. In §2 the accretion rate calculations are described and examined, and §3 presents a scenario that can account for these data. Implications for future observations and the nature of the destroyed and accreted planetary bodies are discussed in §3 and §4.

2 INFERRED ACCRETION RATES FOR DAZ AND DBZ STARS

2.1 Steady State Metal Accretion

If a star is in a steady state between accretion and diffusion, the total mass accretion rate for heavy elements can be expressed as (Dupuis et al. 1993)

$$\dot{M}_z = \sum_i \frac{X_i M_{\text{cvz}}}{\tau_i} \quad (1)$$

where X_i is the mass fraction, τ_i the diffusion (i.e., sinking) timescale for the i^{th} heavy element, and M_{cvz} is the mass of the stellar convection zone or outer atmosphere (defined at the base of the convection zone or at Rosseland optical depth 5, whichever is deeper; Koester 2009). The numerator on the right-hand represents the mass of a the i^{th} element in the convective or outer layers of the star.

All known metal-polluted white dwarfs exhibit the Ca II K line in optical spectroscopy owing to the strength of this atomic transition at this range of effective temperatures (for this reason it is the strongest absorption feature in the Sun). Accretion rate calculations have been naturally tied to this element, and one can derive an accurate infall rate for calcium, and extrapolate to the total mass accretion rate with an appropriate correction factor, as follows

$$\dot{M}_z \approx \frac{1}{A} \frac{X_{\text{Ca}} M_{\text{cvz}}}{\tau_{\text{Ca}}} \quad (2)$$

Prior calculations assumed the infalling material was exactly solar (i.e., including hydrogen and helium;

Koester & Wilken 2006), or 1% solar by mass (i.e., no hydrogen or helium; Jura et al. 2007); the latter yields $A = 1/109.1$ or $1/42.7$ depending on whether the extrapolation is made from a calcium abundance measured as $[\text{Ca}/\text{H}]$ or $[\text{Ca}/\text{He}]$ respectively (Lodders 2003).

2.2 Instantaneous vs. Historical Rates

For $T_{\text{eff}} \gtrsim 11\,000$ K DAZ white dwarfs, Equation 1 can be applied with confidence because these stars possess tiny convection zones or none at all, and have commensurately short metal sinking timescales (on the order of days; Koester 2009) that imply a steady state is virtually certain. Rates computed in this way for warm DAZ stars are ongoing and *instantaneous* measures of the infall of a given heavy element. In contrast, for the coolest DAZ stars and the DBZ stars in general, the assumption of a steady state is uncertain owing to larger diffusion timescales from correspondingly deeper convection zones (Paquette et al. 1986). The DBZ stars can retain atmospheric metals for timescales up to $10^5 - 10^6$ yr, and while they cannot yield instantaneous accretion rates, their sizable convection zones contain the integrated signatures of accretion; a substantial mass of metals acquired within the last few sinking timescales. Because of this, DBZ stars provide a historical record of accretion and, importantly, a minimum mass for the destroyed parent body or bodies (Klein et al. 2010; Farihi et al. 2010a; Jura 2006).

In order to best compare these two classes of polluted stars, Farihi et al. (2009) calculated *historical* accretion rates for DBZ stars; that is, time-averaged over a single diffusion timescale, assuming a steady state. The likelihood of an infrared excess due to circumstellar dust at DAZ stars is correlated with ongoing, high-rate accretion, and thus a similar correlation in the DBZ stars was naturally sought. While the fraction of stars with infrared excess differs between the DAZ and DBZ white dwarfs with accretion rates above a benchmark of $3 \times 10^8 \text{ g s}^{-1}$ (Girven et al. 2012; Xu & Jura 2011; Farihi et al. 2010b, 2009), the relevant point for this study is that until recently, in terms of metal pollution alone and based on the assumption of solar calcium relative to other heavy elements, the two stellar classes appeared to have broadly similar, inferred metal accretion rates.

In what follows, the terms *instantaneous* and *ongoing* are used to refer to accretion rates for warm DAZ stars where a steady state is highly probable, while *historical* and *time-averaged* refer to the rates derived for DBZ stars and the coolest DAZ stars, where an integrated approach is necessary.

2.3 New Accretion Rate Calculations

Assuming 0.01 solar composition by mass, extrapolated from calcium abundance, for both DAZ and DBZ white dwarfs is not ideal, but understandable based on existing data just a couple years prior. However, as discussed in Girven et al. (2012), a more accurate estimation of accretion rates is possible based on recent work. Briefly, there are now eight

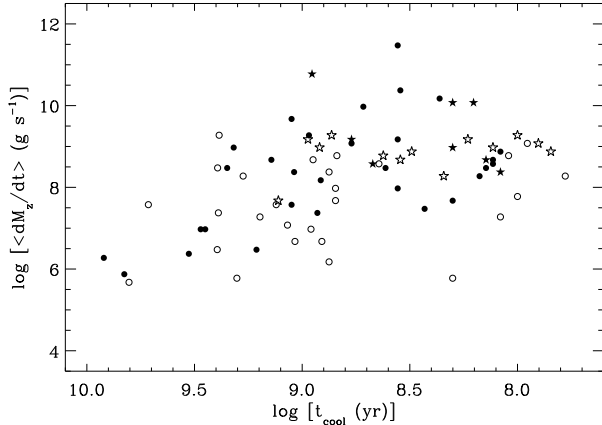


Figure 1. Total metal accretion rates onto 78 contaminated stars observed with *Spitzer* IRAC. The open and filled symbols respectively denote DAZ and DBZ-type white dwarfs, while the stars and circles respectively distinguish those white dwarfs with and without infrared excesses due to circumstellar dust. Among these targets alone there are 8 DBZ stars with accretion rates above the maximum witnessed to be ongoing for any known DAZ white dwarf. Cooling ages are calculated based on white dwarf atmospheric and evolutionary models (Fontaine et al. 2001).

stars with measured O, Mg, Si, Ca, and Fe¹ abundances, with some of these stars exhibiting further elements such as Al, Ti, Cr, and Ni (Gänsicke et al. 2012; Klein et al. 2011; Melis et al. 2011; Farihi et al. 2011a; Zuckerman et al. 2010; Vennes et al. 2010; Dufour et al. 2010; Klein et al. 2010). These data demonstrate that the accreted matter in polluted white dwarfs is broadly similar to rocky material of the inner Solar System. Specifically, Zuckerman et al. (2010) find that calcium represents, on average, close to 1:60 by mass, of all the accreted heavy elements for well-studied stars, while this same ratio is 1:62.5 for the bulk Earth (Allègre et al. 1995).

These results suggest an improved metal accretion rate for dozens of stars where only calcium is detected can be made assuming it is 1.6% ($A = 1/62.5$) of the total mass. Figure 1 plots accretion rates calculated using Equation 2 for 40 DAZ and 38 DBZ stars observed with *Spitzer* IRAC (Girven et al. 2012; Farihi et al. 2010b, 2009, 2008b; Jura et al. 2007). Calcium abundances and stellar parameters come from the most recent studies (e.g., Koester & Wilken 2006), with sinking timescales and convective envelope masses given in Koester (2009). Comparing this plot with those published previously, it is clear there are an increasing number of outlying DBZ-type stars with inferred rates one to a few orders of magnitude above that observed at any DAZ star. Figure 2 re-plots these accretion rates as histograms for both atmospheric types (ignoring dust emission), clearly delineating a subgroup of high values that occur exclusively for DBZ stars. While GALEX 1931+0117 is currently the most extreme example of a DAZ star, with an instantaneous accretion rate of $2 \times 10^9 \text{ g s}^{-1}$ (Gänsicke et al. 2012), its extreme DBZ-type

¹ These elements combined represent over 95% of the bulk Earth (Allègre et al. 1995)

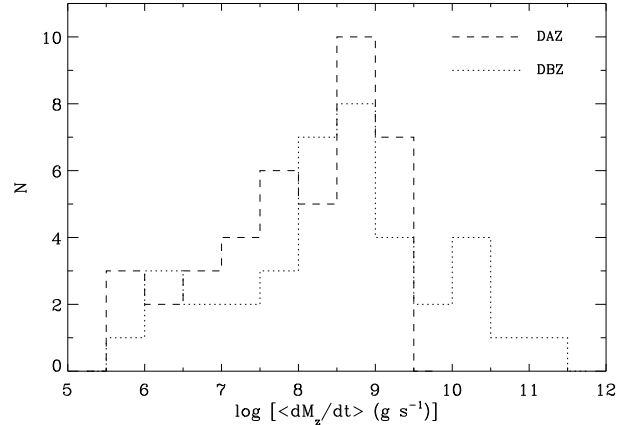


Figure 2. Histogram of the rates plotted in Figure 1 for each atmospheric class of polluted white dwarf. The population of rates $\log(\langle dM_z/dt \rangle \text{ (g s}^{-1}\text{)}) > 9.5$ occur only among the DBZ-type stars.

counterpart is HE 0446–2531 which has a time-averaged rate two orders of magnitude higher at $3 \times 10^{11} \text{ g s}^{-1}$. Figures 1 and 2 plot a large subset of all nearby (pre-SDSS) metal-enriched white dwarfs, but there are additional examples of high rate DBZ stars (e.g., Figure 11 of Xu & Jura 2011), and at least 10 cases where the historical accretion rates are higher than any inferred to be ongoing at DAZ stars.

Table 1 compares accretion rate calculations for the eight stars with robust detections and abundances of O, Mg, Si, Ca, and Fe: in the second column using Equation 2 and assuming calcium is 1.6% of the total accreted metal mass (as described above), and in the third column from the actual detected elements using Equation 1. While a few of these stars exhibit additional elements beyond the five in common, the third column values represent a minimum, as the detection of further elements (e.g., Al, Ni) may serve to increase the calculated rates. However, because most of the major terrestrial elements are detected in these stars, it is possible but unlikely their total accretion rates will change substantially. Comparing the inferred rates from both methods, there is agreement to within ± 0.2 dex for five of the eight stars and overall, while three are over-predicted. These over-predictions may diminish as further elements are detected in these stars, but it is more likely that the (modest) disagreement in the calculated accretion rates are due to real metal-to-metal abundance variations among the parent bodies now falling onto the stars as debris (Zuckerman et al. 2011; Klein et al. 2010).

2.4 Potential Biases

It is worth noting that GALEX 1931 is the only known DAZ star with *optical* detections of all the necessary metals for the Table 1 comparison. This is because, all else being equal, the atmospheric opacity of hydrogen is significantly higher than that of helium (Zuckerman et al. 2003). Because of this, there is a bias against the optical detection of DAZ stars with modest to low amounts of pollution (see Figure 1 of Koester & Wilken 2006 for an excellent illustration of this fact). Within the DA cooling sequence, the combination

of atmospheric opacity and Ca II ionization fraction permits lower metal abundances and accretion rates to be detected at cooler stars. But between the two classes, the detection of metal lines in DA stars is more difficult, favoring those metal-rich stars exhibiting relatively strong lines, and thus high abundances and accretion rates (Koester et al. 2005). *Because the bias works in the opposite direction, the lack of high rates in the DAZ population is real.*

Another possibility is that more vigorous accretion takes place at DBZ stars. However, it is difficult to conjure any scenario that physically favors higher rate accretion of planetary debris at stars with helium atmospheres. There is neither empirical nor theoretical reasoning that suggests the existence of DB stars is related to anything beyond (single) stellar evolution: a very late thermal pulse, immediately following the asymptotic giant phase, can enrich the outer layers of a star with hydrogen-deficient material (Herwig et al. 1999), eventually producing a helium-dominated remnant (Werner & Rauch 1994). Other explanations along these lines would include that DB stars tend to have planetary system architectures more efficient at asteroid perturbation, or parent bodies highly enriched in calcium, but such solutions are contrived and therefore discounted.

Lastly, white dwarf atmospheric models do not have substantial uncertainty in the sizes of the convective or outer envelopes, nor in the gravitational settling behavior at the bottom of these zones (Koester 2009). However, it is feasible that there are gaps in the theoretical understanding of stellar atmospheres that may contribute to the inferred trends, e.g., if the settling times in Equation 1 are systematically under-predicted for DB stars. This possibility is outside of the scope of this paper and not discussed further.

The following sections proceed on the assumption that a planetary system forms without any foreknowledge of the ultimate stellar remnant, and that the planetary bodies within depend only on the conditions at formation and the subsequent influence of stellar evolution and mass loss on those bodies (i.e., only stellar radiation and dynamical changes).

3 A HISTORY OF HIGH ACCRETION RATES

The inescapable conclusion of the data shown in Figure 2 is that there must be relatively short-lived episodes of accretion at metal-polluted white dwarfs; brief enough not to have been observed as ongoing, and at rates substantially higher than those witnessed to date at DAZ stars. This is obviously true for the six stars with time-averaged rates above 10^{10} g s^{-1} , but it also appears likely for the greater DBZ population. Comparing the rates between the DAZ and DBZ groups plotted in the figures, the highest accretion rates differ by a factor of 160, the average of the top six rates differ by a factor of 40, and the average of all the rates differ by a factor of 25. Thus the phenomenon is represented by the entire class of helium atmosphere stars, and accentuated by a handful of outstanding examples.

The rates inferred for the DBZ stars are the mass of accreted metals over a single diffusion timescale, divided by that timescale; around 10^5 yr at 17 000 K and 10^6 yr near 12 000 K (Koester 2009). However, in cases where circumstellar dust is not detected at a given DBZ white dwarf, it

Table 1. Comparison of Accretion Rate Estimates For Stars with Detected O, Mg, Si, Ca, Fe

Star	$\log\langle dM_z/dt(\text{g s}^{-1})\rangle^a$	$\log\langle dM_z/dt(\text{g s}^{-1})\rangle^b$
G241-6	9.8	9.3
GALEX 1931	9.2	9.2
GD 40	10.1	9.4
GD 61	9.0	8.8
HS 2253+8023	10.2	10.1
PG 1015+161	8.5	8.2
SDSS 0738	10.3	10.3
SDSS 1228	9.0	8.8
Log Average	8.66	8.43

^a Assuming Ca is 0.016 of the total accreted mass.

^b From measured abundances of at least O, Mg, Si, Ca, Fe (Gänsicke et al. 2012; Klein et al. 2011; Farihi et al. 2011a; Melis et al. 2010; Vennes et al. 2010; Klein et al. 2010; Dufour et al. 2010; Zuckerman et al. 2010).

Note. The overall differences in the inferred accretion rates between the two columns are minor, and will not affect the findings for DBZ versus DAZ properties; see §2.3 for calculation details.

is possible that accretion halted within the past one to several diffusion timescales. In this sense, the rates inferred for the DBZ stars are *minimum*, time-averaged rates, as atmospheric metal abundances will exponentially diminish, but remain potentially detectable for a few to several sinking timescales after accretion has ended. For simplicity, the following assumes all observed metals are accreted over a single diffusion timescale; if accretion is no longer ongoing, then prior accretion must have occurred at even higher rates than those inferred below.

3.1 High and Low State Model

For a toy model with two distinct and constant accretion rates – a high state and a low state – taking place over a single diffusion timescale for a typical DBZ star, the observed mass of metals in the stellar convection zone M_z can be written as:

$$\dot{M}_z \tau = \dot{M}_h t_h + \dot{M}_l t_l \quad (3)$$

where t_h/τ is the fraction of time the star is accreting at the high rate \dot{M}_h , similarly t_l/τ is the fraction of time spent accreting at the low rate \dot{M}_l , and where τ is the diffusion timescale. The right hand side of Equation 3 simply breaks the total accreted mass into that delivered in two distinct states, but one can easily extend this to a continuum of rates and corresponding intervals; this does not change the conclusions reached here. As shown in §3.2, since $t_h \ll t_l$, it follows that $t_l \sim \tau$ and thus t_h/t_l is the fraction of the total time spent accreting in the high state. This allows for the possibility that \dot{M}_h occurs in a succession of episodes, not just one per DBZ diffusion timescale. The mass represented by both sides of Equation 3 is typically 10^{22} g for a given DBZ star, but this can vary by up to two orders of magnitude (Girven et al. 2012; Farihi et al. 2010a).

Identifying τ and \dot{M}_z as the diffusion timescale and time-averaged accretion rate for DBZ-type stars, and equat-

Table 2. Accretion Rates for Figure 3

Line	DBZ stars $\log(\dot{M}_z [\text{g s}^{-1}])$	DAZ stars $\log(\dot{M}_l [\text{g s}^{-1}])$	Description
Dash	11.5	9.3	Max \dot{M}
Long Dash	10.8	9.2	Top 6 \dot{M}
Solid	10.1	8.7	Avg \dot{M}

Note. There are six DBZ stars with inferred accretion rates above 10^{10} g s^{-1} (see Figure 2).

ing \dot{M}_l to that measured for the DAZ white dwarfs, Equation 3 permits the assessment of (t_h, \dot{M}_h) values sufficient to account for the inferred differences among the instantaneous and historical accretion rates. Figure 3 plots three representative solutions for $\tau = 10^6 \text{ yr}$, with parameters described in Table 2. From top to bottom are plotted the resulting (t_h, \dot{M}_h) for pairs of \dot{M}_z and \dot{M}_l representing 1) the single highest accretion rates in each class, 2) the average of the top six rates in each class, and 3) the average among all stars in each class from Figure 1.

3.2 Allowed Timescales for High Rate Episodes

Because ongoing accretion rates as high as those inferred for the DBZ have not been witnessed to date, strict limits can be placed on the timescales for such episodes, t_h . For $\tau = 10^6 \text{ yr}$ and a high-rate accretion timescale of $t_h = 10^5 \text{ yr}$ ($0.11t_l$), the probability that at least one of 46 known DAZ stars will be accreting at the high rate is above 99%, while for $t_h = 10^4 \text{ yr}$ ($0.01t_l$) this same probability drops to 37%. Based on this argument alone, one can conclude $t_h \ll t_l$, and the timescale for any high-rate episodes must be no more than 10^4 yr . Moreover, a few of the most highly polluted DBZ stars have $\tau \sim 10^5 \text{ yr}$ (e.g., GD 362, Ton 345), which supports even shorter timescales for high-rate spikes.

Notably, DA stars without detected metals constrain t_h more strongly. The high-resolution spectroscopic studies of Zuckerman et al. (2003) and Koester et al. (2005) collectively surveyed approximately 530 DA white dwarfs for photospheric metals, where stars more highly polluted than GALEX 1931 would have been readily detected. It is also likely that extreme metal abundances in DA white dwarfs are identifiable in the low-resolution spectra of the Sloan Digital Sky Survey; SDSS 1228 is one of the most metal-rich DAZ stars and its discovery spectrum exhibits a clear Mg II absorption line at $g = 16.2 \text{ AB mag}$ (Gänsicke et al. 2006). While this star is relatively bright among the few thousand spectroscopically confirmed DA white dwarfs identified in SDSS DR7, there are nearly 470 DA stars with $g < 17.0 \text{ AB mag}$ where very high metal abundances (and thus accretion rates) were not detected (Girven et al. 2011). Based on these surveys, it is likely that $t_h < 10^3 \text{ yr}$.

3.3 Rapid Accretion of Gaseous Debris

Using the α prescription (King et al. 2007) for completely gaseous accretion disks, Jura (2008) estimates that a disk composed purely of metallic gas will dissipate within 10^5 yr , for $\alpha = 0.001$. While this timescale is longer than the allowed range of t_h in Figure 3, below it is shown that a reasonable

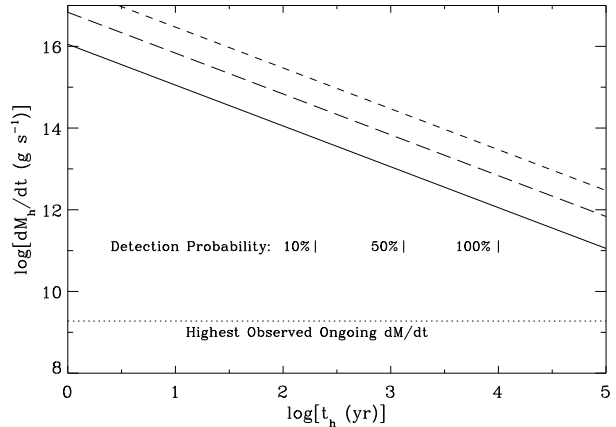


Figure 3. Necessary (t_h, \dot{M}_h) that satisfy Equation 3 for $\tau = 10^6 \text{ yr}$, and Table 2 values for \dot{M}_z and \dot{M}_l . It should be noted that there is little difference in the plotted lines and those that result from $\dot{M}_l = 0$. Also shown are resulting benchmark probabilities of detecting high states of marked durations, given the sample of 534 DA stars surveyed at high resolution with Keck and VLT (Koester et al. 2005; Zuckerman et al. 2003). Episodes of high rate accretion lasting tens to hundreds of years are allowed, while if the timescales approaches or exceeds 10^3 yr then the likelihood of detection at DAZ stars increases towards unity. This result is corroborated by the lack of extremely polluted DAZ stars in the SDSS DR7 (Girven et al. 2011).

choice of α can produce both t_h and \dot{M}_h values necessary to account for the accretion rate data.

The accretion rate of a completely gaseous disk can be expressed as

$$\dot{M} = \frac{m}{t_\nu} \quad (4)$$

where m is the mass of the disk and t_ν is the viscous timescale at a distance d from the central star

$$t_\nu = \frac{d^2}{\nu} \quad (5)$$

The viscosity ν can be rewritten following the α prescription (Pringle 1981) and Equation 5 becomes

$$t_\nu = \frac{p}{\alpha} \left(\frac{d}{h} \right)^2 \quad (6)$$

where p is the orbital period and h is the scale height of the disk. For an ideal, isothermal gas orbiting a star of mass M at a distance d , the scale height is (Pringle 1981):

$$h = \sqrt{\frac{kT d^3}{GM\mu}} \quad (7)$$

where T is the temperature of gas with mean molecular weight μ .

Metallic, circumstellar gas has been modeled at temperatures around 6000 K in the few, well-studied stars with calcium triplet emission lines, using three independent means (Hartmann et al. 2011; Melis et al. 2010; Gänsicke et al. 2006). Gas composed of singly ionized O, Mg, Si, Fe will have a mean particle mass $\mu = 2.5 \times 10^{-23} \text{ g}$, and if this orbits at $0.5 R_\odot$ about a $0.6 M_\odot$ white dwarf, then $d/h \approx 260$.

Then the viscous timescale at this distance becomes $t_\nu \approx (10/\alpha)$ yr and in the range 25 to 100 yr for $\alpha = 0.1 - 0.4$; typically required to account for observational data in a wide variety of fully ionized disks (King et al. 2007). This viscous timescale is consistent with observations in two ways: 1) it is sufficiently short as to remain currently undetected at DAZ stars, and 2) for the largest, accreted metal masses in DBZ star convection zones (10^{24} g; Girven et al. 2012; Farihi et al. 2010a), it implies rates up to 10^{15} g s $^{-1}$ (and higher for smaller d).

Metal-rich, pure gas disks at such temperatures will be highly or fully (singly) ionized as their overall ionization potential will be lower than similar accretion disks of solar abundance, hydrogen-dominated material². Thus, a disk of gaseous metals will be conductive, stable, and the standard α should hold (Stone et al. 2000; Gammie & Menou 1998). Accretion of gaseous debris via viscous dissipation with $\alpha = 0.1 - 0.4$ thus nicely accounts for the data in Figure 2, yielding the correct range of rates and timescales dictated by Figure 3, and is hence plausible.

Two recent studies have also shown that short bursts of high rate accretion are possible from disrupted asteroids at white dwarfs. Rafikov (2011b) demonstrates that, under certain conditions, gas may efficiently couple with solids and lead to the inward drift of particulate disk matter at rates greatly exceeding that of Poynting-Robertson forces. In this scenario, a spike of maximal accretion occurs at the very end of a disk episode (Metzger et al. 2012). In contrast, Bear & Soker (2012) show that a Nova-like, accretion-driven outburst may occur during the initial phases of an asteroid disruption and disk formation. The standard α disk model used here applies to any epoch where sufficient gas is produced, and overlaps with these other models under appropriate conditions.

3.4 Generating Asteroid-Sized Masses in Gas

This section considers the efficient vaporization of significant masses of solid matter originally contained in extrasolar asteroids; i.e., processes able to reproduce the rates deduced in the previous sections. Such gas production must be orders of magnitude more vigorous than sublimation of dust at the inner edge of a flat disk (see §3.5), as this cannot produce the sufficiently high infall rates dictated by the accretion histories represented by Figure 3. The following should be considered for heuristic purposes only.

One possibility is a planetesimal impinging on a pre-existing disk from the prior asteroid disruptions, as investigated in detail by Jura (2008). In that model, if the incoming asteroid is less massive than the disk, its entire debris mass is reduced to gas via collisions and sputtering, while if it is more massive, then the disk mass is vaporized and the excess asteroid mass persists in solids. Both cases have the potential to produce a large asteroid mass of gaseous debris and allow for the possibility that a disk of solids will remain. The metal-enriched white dwarfs G166-58 and PG 1225-079 both appear to have dust rings with enlarged inner holes

(Farihi et al. 2010b, 2008b), where an impact may have destroyed the inner region solids but left the outer disk intact.

A second scenario is a lone tidal disruption event. A planetesimal will be shredded on its first approach, but the fragments will simply continue along their eccentric orbits (i.e., none will impact the star), dispersed but tightly centered around the original orbit of the parent body, analogous to stellar disruptions at black holes (Lodato et al. 2009; Rosswog et al. 2009). The pieces will be sufficiently small as to be immune to tidal gravity, but will collide at periastron on subsequent passes. Such collisions will occur at high relative velocity and so can generate gas (Tielens et al. 1994) as well as dust. Furthermore, solid debris will be prone to sublimation while not yet shadowed by a disk, as optically thin material is heated above 1200 K within $1.0 R_\odot$ (the approximate Roche limit) of a typical 15 000 K white dwarf. These modes of gas production will eventually abate, as eccentric motion damping reduces collisional velocities and particles become shadowed by a growing (flat) disk of material. The complete reduction of an asteroid into a disk will likely take many orbital periods; e.g., taking the 11.8 yr orbital period of Jupiter as a benchmark, one would expect planetesimals perturbed from orbits at similar distances from their host stars will take hundreds of years to make several passes.

The timescale for particle collisions in an optically thin disk within the Roche limit of a cool white dwarf is typically shorter than Poynting-Robertson drag timescale by an order of magnitude (but with a linear dependence on optical depth and particle size; Farihi et al. 2008a). In this regime, planetesimal debris generated by tidal disruption can only be reduced by collision or sublimation, at least until the disk becomes optically thick, at which point the disk evolution will be dominated by Poynting-Robertson drag at the inner edge, and viscous forces elsewhere (Rafikov 2011a). Disk observations that reveal 1) silicate emission features in the mid-infrared (Jura et al. 2009; Reach et al. 2009) and 2) radially coincident gas and dust at some polluted white dwarfs (Farihi et al. 2012; Melis et al. 2010; Brinkworth et al. 2009; Gänsicke et al. 2008, 2007, 2006) are consistent with a picture whereby the shattered parent body is at least partially (if not totally) reduced to micron-sized and smaller particles. It is therefore plausible that a significant gaseous mass will result from the initial phases of a tidal disruption event.

3.5 Observational Consequences and Predictions

This rapid gas accretion scenario has implications for observations of circumstellar disks and metal-polluted white dwarfs. Perhaps most notably, those stars suspected to be accreting gaseous debris *alone* should exhibit the highest rates, and far exceed the Poynting-Robertson drag rates for white dwarfs. Ultimately, all material falling onto the stellar surface will be in gas phase, and circumstellar disks may have 1) a cool outer region dominated by solids, 2) a narrow transition region where solids and gas coexist, and 3) a hot inner region where all debris is sublimated. Such architecture is inferred for the dust disks found and characterized by *Spitzer* (e.g., Farihi et al. 2009; Jura et al. 2007; von Hippel et al. 2007, and the limiting factor in their infall rates is the (solid) mass per unit time delivered to the edge of the sublimation zone by Poynting-Robertson forces (Rafikov 2011a). Once vaporized, the model presented here predicts

² Of the expected major elements in a disk of vaporized rock, only O I has an ionization potential comparable to H I.

that gaseous accretion takes place on short timescales, but will produce very different infall rates for disks whose total mass is dominated by solids, and those dominated by gas.

Based on the above, those disks detected to have spatially coincident dust and gas (six are known at present: Brinkworth et al. 2012; Dufour et al. 2012; Melis et al. 2012; Farihi et al. 2012; Melis et al. 2010; Brinkworth et al. 2009) are likely to be dominated by solids. Critically, the best observations to date indicate that the (calcium) gas emission drops off sharply at the inner orbital radius where the particulate disk is modeled to terminate (Melis et al. 2010; Brinkworth et al. 2009). These data are consistent with the rapid depletion of a completely gaseous inner region, resulting in a relatively low surface density, a corresponding lack of detected emission, and are compatible with the model presented here.

Notably, observations reveal that white dwarfs with detectable dust disks have, on average, the highest ongoing accretion rates. Figure 4 plots a histogram of metal accretion rates for DAZ stars with and without infrared excesses from circumstellar disks. While essentially no stars exceed the range of infall rates expected for Poynting-Robertson drag, the stars without obvious dust are the slowest accretors. Many of the DAZ without infrared excess are sufficiently warm that they must be accreting unseen material; either gaseous or tenuous dust disks (Farihi et al. 2010b). The picture presented here predicts these stars are indeed accreting from undetected particulate disks, rather than purely gaseous matter, but it is also plausible that α varies substantially between gas disks (Jura 2008). More sensitive infrared observations can test this prediction.

Detailed spectroscopy of DBZ white dwarfs has the potential to constrain the frequency of events that produce significant masses of gaseous debris, or distinct pollution events more generally. For a given baseline of exo-chondritic or -terrestrial compositions, the heaviest elements such as iron and nickel should be under-abundant in DBZ stars if the timescale for major asteroid incursions is longer than the lifetime of photospheric metals. To date there is a mix of observational results: there appear to be two white dwarfs polluted by intrinsically iron-poor material (Zuckerman et al. 2011; Farihi et al. 2011a), while most iron-deficient stars are consistent with gravitational settling (Koester et al. 2011; Farihi et al. 2011b). Analysis of a large number of DBZ (and very cool DAZ) stars is needed to better understand these abundance patterns, as it remains possible that extrasolar, solid planetary material can be distinct from that contained in any known (or modeled) rocky bodies. But it is plausible that certain abundance patterns can only be maintained if discrete, substantial pollution events occur on timescales shorter than the heavy element lifetimes in typical DBZ stars.

It is noteworthy that the toy model of high and low accretion states, which is certainly an approximation of reality, underscores the quasi-steady state accretion model recently outlined by (Jura & Xu 2012). In that model, the heavy element abundances observed in the atmospheres of DBZ-type white dwarfs may differ substantially from both the steady state and early phase models (Koester 2009). Under certain conditions, parent body chemical abundances can be uncertain by a factor of two in mass. The results presented here constrain r , but not ω in Equation 10 of Jura & Xu (2012).

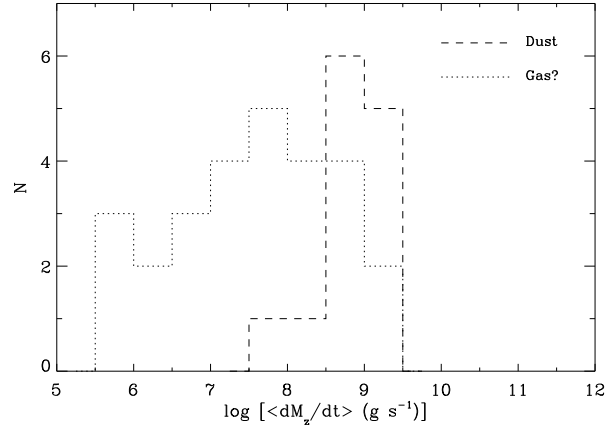


Figure 4. Accretion rates for the 40 DAZ stars in Figure 1. The dashed and dotted histograms show stars with and without an infrared excess, respectively. Among 19 stars with $T_{\text{eff}} \gtrsim 10\,000\text{K}$ and where ongoing accretion is highly probable, 11 stars accreting from dust disks have an average infall rate more than three times higher than eight stars that lack infrared excesses. If these latter stars accrete from gas-dominated circumstellar disks (Jura 2008), the difference in inferred accretion rates would be contrary to the predictions made here, which suggest that pure gas disks achieve the highest accretion rates, whereas solid-dominated disks are limited by Poynting-Robertson forces (Rafikov 2011a).

3.6 Total Mass Accreted in High State

An important consequence of the proposed scenario is the necessary mass (in gaseous heavy elements) delivered during the high state accretion episodes, and specifically the total mass accreted within t_h so that its signature is still visible today among the DBZ population. The required mass depends on the choice of constants in Equation 3, but for $\tau = 1\text{ Myr}$ a mass of $\dot{M}_h t_h \sim 10^{23}\text{ g}$ will reproduce the average DBZ accretion rates, for \dot{M}_l equal to the average DAZ rate; this solution is represented by solid line in Figure 3. If instead the diffusion timescale for the DBZ stars is taken to be 10^5 yr or smaller (as for GD 362 and Ton 345), then the necessary mass decreases to the order 10^{22} g .

If a second planetary body is perturbed to collide with a pre-existing disk system, then the gaseous debris mass needed to satisfy the above criteria is about that of Vesta, conservatively speaking. The largest asteroids in the Solar System – Ceres, Vesta, and Pallas – are best described as intact planetary embryos, and while their sizes and masses are exceptional even among the largest objects in the Main Belt members, such masses may be more commonplace among planetesimals formed at the intermediate mass, A- and F-type progenitors of typical, extant white dwarfs. If the entire mass is not converted to gas when a second body impacts a disk, and remaining material is gradually delivered to the star in a particulate disk, then a Vesta analog represents the minimum mass necessary to account for the data.

In the case where singular events are the cause of metal-enriched white dwarfs, and substantial gas mass is only produced immediately following a tidal disruption, the parent bodies must be larger still. Again for the criteria above, one needs 10% of a 10^{24} g or 1% of a 10^{25} g parent body to be accreted within a 100 yr period, as gas, with the remaining

mass gradually delivered to the star in a particulate disk, at the rates observed for the DAZ stars. Here the parent bodies would be at least massive as Ceres, and perhaps as large as Pluto. Also, the particulate disk lifetimes necessary to accrete the remaining mass at more modest rates exceed 10^6 yr. Neither of these predictions is a priori unreasonable, and further observations and modeling may help to constrain these quantities.

4 CONCLUSIONS

The rapid infall of gaseous debris at white dwarfs can account for the difference between the currently observed and ongoing metal accretion rates at DAZ stars and the time-averaged, historical rates inferred for the DBZ stars. The data constrain the lifetime of the necessary, high-rate accretion episodes to be strictly less than 10^4 yr, and gas disk models with $\alpha \sim 0.1$ can achieve rates approaching or exceeding 10^{15} g s $^{-1}$; sufficient to consume Vesta in 10 yr. The several hundred DA white dwarfs surveyed for metals suggest that the high-rate accretion timescale is likely less than 10^3 yr, while a search of $\sim 10\,000$ DA stars is necessary to confidently detect one in a high state that lasts ~ 100 yr.

Such rapid accretion is not unrealistic and within an order of magnitude of the highest accretion rates found for cataclysmic variables in quiescence (Baskill et al. 2005 2005; Gänsicke et al. 1995). Given that *ROSAT* was capable of detecting x-ray luminosities as low as 10^{30} erg s $^{-1}$ at distances beyond 100 pc (Pretorius & Knigge 2012), corresponding to accretion rates of 10^{13} g s $^{-1}$ for typical $0.6 M_{\odot}$ white dwarfs, it is likely that near-future facilities will detect the high-rate accretion episodes predicted here, if the model is accurate (see Bear & Soker 2012 for alternative predictions). *eROSITA* will be a factor of 100 times more sensitive than *ROSAT* in the $0.5 - 2$ keV band³, meaning that accretion rates as low as 10^{11} g s $^{-1}$ may be detectable within a few hundred pc. Moreover, wide-field and high-cadence surveys such as LSST and Pan-Starrs may detect optical transients associated with these events. Lastly, *GAIA* should be capable of identifying a single white dwarf accreting in a high state, as it should identify 10^6 white dwarfs and thus yield at least 10 000 metal-polluted stars. These data will help to constrain t_h and \dot{M}_h .

A readily testable hypothesis is that all relatively warm DAZ stars accreting near or below Poynting-Robertson drag rates are accreting from particulate, not gaseous, debris disks. Farihi et al. (2010b) has shown that narrow rings of dust exist at some polluted white dwarfs, and that 10^{22} g can easily be missed in photometric surveys for infrared excess. Those DAZ stars without obvious infrared excess in *Spitzer* IRAC photometry may reveal dust with higher sensitivity observations. High signal-to-noise spectroscopy over the $5 - 15 \mu\text{m}$ range, where both thermal and silicate emission are salient for disks observed to date (Reach et al. 2009; Jura et al. 2009), is perhaps the ideal choice for the detection of subtle infrared excesses at white dwarfs. This would be somewhat analogous to the identification of dust

at HD 69830 (Lisse et al. 2007), where the fractional infrared luminosity is relatively low.

If the accretion of gaseous debris delivers significant mass to metal-contaminated white dwarfs, the destroyed and devoured parent bodies must be at least as massive as the largest Solar System asteroids, and possibly comparable in mass to the largest moons. Such objects will be differentiated, consistent with the few polluted white dwarfs with detailed abundance measurements for major elements of planetary solids. The overall results show that quasi-steady state accretion may be important, and models that constrain the frequency of high accretion states will strengthen the analytical connection between the observed stellar abundances and the chemistry of planetary debris at DBZ and very cool DAZ white dwarfs.

ACKNOWLEDGMENTS

The authors thank the anonymous referee for feedback which improved the quality and clarity of the manuscript.

REFERENCES

- Allegre C. J., Poirier J. P., Humler E., Hofmann A.W. 1995, *Earth Planetary Sci. Letters*, 4, 515
 Baskill D. S., Wheatley P. J., Osborne J. P. 2005, *MNRAS*, 357, 626
 Bear E., Soker N. 2012, arXiv:1203.2726
 Bonsor A., Mustill A. J., Wyatt M. 2011, *MNRAS*, 414, 930
 Brinkworth C. S., Gänsicke B. T., Marsh T. R., Hoard D. W., Tappert C. 2009, *ApJ*, 696, 1402
 Brinkworth C. S., Gänsicke B. T., Girven J., Hoard D. W., Marsh T. R., Parsons S. G., Koester D. 2012, *ApJ*, 750, 86
 Chayer P., Fontaine G., Wesemael F. 1995, *ApJS*, 99, 189
 Debes J. H., Sigurdsson S. 2002, *ApJ*, 572, 556
 Debes J., Walsh K., Stark C. 2012, *ApJ*, 747, 148
 Dufour P., Kilic M., Fontaine G., Bergeron P., Lachapelle F. R., Kleinman S. J., Leggett S. K. 2010, *ApJ*, 719, 803
 Dufour P., Kilic M., Fontaine G., Bergeron P., Melis C., Bochanski J. 2012, *ApJ*, 749, 6
 Dufour P., et al. 2007, *ApJ*, 663, 1291
 Dupuis J., Fontaine G., Pelletier C., Wesemael F. 1993, *ApJS*, 84, 73
 Farihi J., Brinkworth C. S., Gänsicke B. T., Marsh T. R., Girven J., Hoard D. W., Klein B., Koester D. 2011a, *ApJ*, 728, L8
 Farihi J., Becklin E. E., Zuckerman B. 2005, *ApJS*, 161, 394
 Farihi J., Becklin E. E., Zuckerman B. 2008a, *ApJ*, 681, 1470
 Farihi J., Barstow M. A., Redfield S., Dufour P., Hambly N. C. 2010a, *MNRAS*, 404, 2123
 Farihi J., Gänsicke B. T., Steele P. R., Girven J., Burleigh M. R., Breedt E., Koester D. 2012, *MNRAS*, 421, 1635
 Farihi J., Jura M., Lee J. E., Zuckerman B. 2010b, *ApJ*, 714, 1386
 Farihi J., Jura M., Zuckerman B. 2009, *ApJ*, 694, 805
 Farihi J., Dufour P., Napiwotzki R., Koester D. 2011b, *MNRAS*, 413, 2559

³ <http://www.mpe.mpg.de/erosita/science.php?lang=en>

- Farihi J., Zuckerman B., Becklin E. E. 2008b, *ApJ*, 674, 431
- Fontaine G., Brassard P., Bergeron P. 2001, *PASP*, 113, 409
- Fontaine G., Michaud G. 1979, *ApJ*, 231, 826
- Gammie C. F., Menou K. 1998, *ApJ*, 492, L75
- Gänsicke B. T., Beuermann K., de Martino D. 1995, *A&A*, 303, 127
- Gänsicke B. T., Koester D., Marsh T. R., Rebassa-Mansergas A., Southworth J. 2008, *MNRAS*, 391, L103
- Gänsicke B. T., Koester D., Farihi J., Girven J., Parsons S. G., Breedt E. 2012, *MNRAS*, in press
- Gänsicke B. T., Marsh T. R., Southworth J. 2007, *MNRAS*, 380, L35
- Gänsicke B. T., Marsh T. R., Southworth J., Rebassa-Mansergas A. 2006, *Science*, 314, 1908
- Girven J., Brinkworth C. S., Farihi J., Gänsicke B. T., Hoard D. W., Marsh T. R., Koester D. 2012, *ApJ*, 749, 154
- Girven J., Gänsicke B. T., Steeghs D., Koester D. 2011, *MNRAS*, 417, 1210
- Graham J. R., Matthews K., Neugebauer G., Soifer B. T. 1990, *ApJ*, 357, 216
- Hartmann S., Nagel T., Rauch T., Werner K. 2011, *A&A*, 530, 7
- Herwig F., Blöcker T., Langer N., Driebe T. 1999, *A&A*, 349, L5
- Holberg J. B., Bergeron P. 2006, *AJ*, 132, 1221
- Jura M. 2003, *ApJ*, 584, L91
- Jura M. 2006, *ApJ*, 653, 613
- Jura M. 2008, *ApJ*, 135, 1785
- Jura M., Farihi J., Zuckerman B. 2007, *ApJ*, 663, 1285
- Jura M., Farihi J., Zuckerman B. 2009, *AJ*, 137, 3191
- Jura M., Xu S. 2012, *AJ*, 143, 6
- Klein B., Jura M., Koester D., Zuckerman B., Melis C. 2010, *ApJ*, 709, 950
- Klein B., Jura M., Koester D., Zuckerman B. 2010, *ApJ*, 741, 64
- King A., Pringle J., Livio M. 2007, *MNRAS*, Koester D. 2009, *A&A*, 498, 517
- Koester D., Girven J., Gänsicke B. T., Dufour P. 2011, *A&A*, 530, 114
- Koester D., Rollenhagen K., Napiwotzki R., Voss B., Christlieb N., Homeier D., Reimers D. 2005, *A&A*, 432, 1025
- Koester D., Wilken D. 2006, *A&A*, 453, 1051
- Lanz T., Hubeny I. 1995, *ApJ*, 439, 875
- Lisse C. M., Beichman C. A., Bryden G., Wyatt M. C. 2007, *ApJ*, 658, 584
- Lodato G., King A. R., Pringle J. E. 2009, *MNRAS*, 392, 332
- Lodders K. 2003, *ApJ*, 591, 1220
- Melis C., Jura M., Albert L., Klein B., Zuckerman B. 2010, *ApJ*, 722, 1078
- Melis C., Farihi J., Dufour P., Zuckerman B., Burgasser A. J., Bergeron P., Bochanski J., Simcoe R. 2011, *ApJ*, 732, 90
- Melis C., Dufour P., Bochanski J., Burgasser A. J., Parsons S. G., Gänsicke B. T., Farihi J., Koester D., Swift B. J. 2012, *ApJ*, submitted
- Metzger B. D., Rafikov R. R., Bochkarev K. V. 2012, *MNRAS*, in press (arXiv:1202.0557)
- Paquette C., Pelletier C., Fontaine G., Michaud G. 1986, *ApJS* 61, 197
- Pretorius M. L., Knigge C. 2012, *MNRAS*, 419, 1442
- Pringle J. E. 1981, *ARA&A*, 19, 137
- Rafikov R. R. 2011a, *ApJ*, 732, L3
- Rafikov R. R. 2011b, *MNRAS*, 416, L55
- Reach W. T., Kuchner M. J., von Hippel T., Burrows A., Mullally F., Kilic M., Winget D. E. 2005, *ApJ*, 635, L161
- Reach W. T., Lisse C., von Hippel T., Mullally F. 2009, *ApJ*, 693, 697
- Rosswog S., Ramirez-Ruiz E., Hix W. R. 2009, *ApJ*, 695, 404
- Sion E. M., Hammond G. L., Wagner R. M., Starrfield S. G., Liebert J. 1990, *ApJ*, 362, 691
- Stone J. M., Gammie C. F., Balbus S. A., Hawley J. F., Boss A. P., Russell S. S. (Univ. Arizona Press: Tucson), 589
- Tielens A. G. G. M., McKee C. F., Seab C. G., Hollenbach D. J. 1994, *ApJ*, 431, 321
- van Maanen A. 1917, *PASP*, 29, 258
- Vennes, S., Kawka, A., Németh, P. 2010, *MNRAS*, 404, L40
- von Hippel T., Kuchner M. J., Kilic M., Mullally F., Reach W. T. 2007, *ApJ*, 662, 544
- Werner K., Rauch T. 1994, *A&A*, 284, L5
- Xu S., Jura M. 2011, *ApJ*, 745, 88
- Zuckerman B., Koester D., Reid I. N., Hüensch M. 2003, *ApJ*, 596, 477
- Zuckerman B., Koester D., Melis C., Hansen B. M. S., Jura M. 2007, *ApJ*, 671, 872
- Zuckerman B., Melis C., Klein B., Koester D., Jura M. 2010, *ApJ*, 722, 725
- Zuckerman B., Koester D., Dufour P., Melis C., Klein B., Jura M. 2011, *ApJ*, 739, 101